

Numerical Study of Turbulent Spray Combustion within the Reverse Flow Combustor of a Turbo shaft Engine

G. Öztarlık¹, and O. Tuncer²

¹*Research & Development Department, TUSAŞ Engine Industries, Tepebaşı, 26003, Eskişehir, Turkey, gorkem.oztarlik@gmail.com*

²*Faculty of Aeronautics and Astronautics, Istanbul Technical University, Department of Aeronautical Engineering, 34469, Maslak, Istanbul, Turkey, tuncero@itu.edu.tr*

Abstract – This study presents numerical simulation of turbulent spray combustion within the planar sector for a 1000-hp class turbo-shaft engine reverse flow combustor. Simulation domain with three swirler cups corresponds to a sector of a full annular combustor and the grid also includes the annulus flow. A coupled Euler-Lagrange method models the two-phase reacting flow wherein chemistry and turbulence interaction is accounted for by the Eddy Dissipation Concept Model. Random Walk model is used to model the interaction between continuous and disperse phases. Combustion is modeled with a single step global reaction and its rate is limited by the Eddy Dissipation Concept Model. Results indicate the presence of hot spots at the exit plane at locations just across the injectors. The simulation suggests that some dilution jets over penetrate the cross flow with trajectories close to the liner across. This indicates the necessity for design iteration.

1. Introduction

Turbulent spray combustion is used in many practical devices and aero-engines are one of them. This is a fairly complex flow situation wherein a two-phase reacting flow consisting of combustion gasses and fuel droplets interacts with turbulence, which modifies both fluid and droplet transport.

The case investigated in this study is a planar sector with three radial swirler assemblies operating at reduced atmospheric conditions for take-off regime. The fuel is injected into the swirler assembly via the pressure-swirl atomizer, where droplet heat-up/evaporation takes place at the same time [1].

The swirler mixes the fuel and air, forming a heterogeneous mixture of fuel droplets and combustible fresh gasses, which is then transported into the combustion chamber where it is continuously self-ignited by the combustion products residing in the recirculation bubble [2].

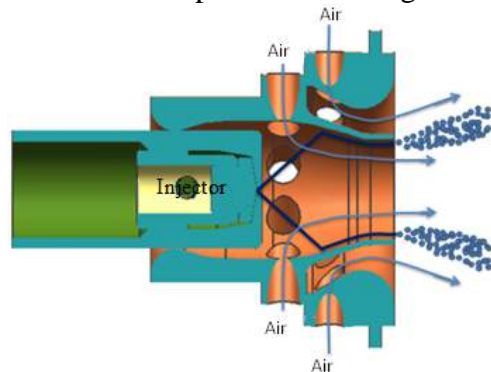


Figure 1: Schematic representation of the swirler assembly.

The main intention behind these simulations is to gain approximate insight into the averaged temperature field which in turn is used in preliminary design studies for cooling implementation. Since the fuel is fed with a spray, the flame is considered to be a diffusion flame and temperatures are expected to be close to equilibrium temperature at some point in the flow as a result of mixing.

2. Mathematical Model

An Eulerian-Lagrangian approach was used to model the two phases of liquid fuel droplets and the combustion gasses. Numerical simulations are performed using the ANSYS Fluent CFD package on a parallel computing cluster.

2.1. Eulerian Phase Modeling

The turbulence model employed is the realizable $k - \epsilon$ model along with scalable wall functions. Combustion is modeled using Eddy Dissipation Model brought up by Magnussen which uses the assumption that reactions takes place in fine structures with characteristic dimensions of the order of Kolmogorov length scale [3].

Mass, momentum, species and energy conservation equations are provided in Eq. 1 through Eq. 4.

$$\frac{\partial \bar{\rho}}{\partial t} + \frac{\partial}{\partial x_i} (\rho \tilde{u}_i) = \bar{S}_{Mass} \quad (1)$$

$$\frac{\partial}{\partial t} (\bar{\rho} \tilde{u}_i) + \frac{\partial}{\partial x_j} (\bar{\rho} \tilde{u}_i \tilde{u}_j) = -\frac{\partial \bar{p}}{\partial x_i} + \frac{\partial}{\partial x_j} \left[\mu \left(\frac{\partial \tilde{u}_i}{\partial x_j} + \frac{\partial \tilde{u}_j}{\partial x_i} - \frac{2}{3} \delta_{ij} \frac{\partial \tilde{u}_l}{\partial x_l} \right) \right] + \frac{\partial}{\partial x_j} \left(\mu_t \left(\frac{\partial \tilde{u}_i}{\partial x_j} + \frac{\partial \tilde{u}_j}{\partial x_i} \right) - \frac{2}{3} (\bar{\rho} \tilde{k} + \mu_t \frac{\partial \tilde{u}_k}{\partial x_k}) \delta_{ij} \right) + \bar{S}_{Mom,i} \quad (2)$$

$$\frac{\partial}{\partial t} (\bar{\rho} \tilde{Y}_k) + \frac{\partial}{\partial x_i} (\bar{\rho} \tilde{u}_i \tilde{Y}_k) = \frac{\partial}{\partial x_i} \left[\left(\bar{\rho} \bar{D}_{i,m} + \frac{\mu_t}{Sc_t} \right) \frac{\partial \tilde{Y}_k}{\partial x_i} \right] + \bar{R}_i + \bar{S}_i \quad (3)$$

$$\frac{\partial}{\partial t} (\bar{\rho} \tilde{E}) + \frac{\partial}{\partial x_i} (\tilde{u}_i (\bar{\rho} \tilde{E} + \bar{p})) = \frac{\partial}{\partial x_j} \left(k_{eff} \frac{\partial \tilde{T}}{\partial x_j} - \sum_j \tilde{h}_j \left(-\bar{\rho} \bar{D}_{j,m} + \frac{\mu_t}{Sc_t} \right) \frac{\partial \tilde{Y}_i}{\partial x_i} - \bar{D}_{T,j} \frac{\partial \tilde{T}}{\partial x_i} \right) + \bar{S}_R + \bar{S}_D \quad (4)$$

Total enthalpy E and species enthalpies h_i are computed according to Eq. 5 and Eq. 6 respectively.

$$\tilde{E} = \sum_j \tilde{Y}_j \tilde{h}_j + \frac{|\tilde{V}|^2}{2} \quad (5)$$

$$\tilde{h}_j = \int_{T_{ref}}^T c_{p,j} d\tilde{T} \quad (6)$$

Realizable k-e model is used to model turbulence. Eq.7 and Eq. 8 are transport equations for turbulent kinetic energy and its dissipation respectively.

$$\frac{\partial}{\partial t} (\bar{\rho} \tilde{k}) + \frac{\partial}{\partial x_j} (\bar{\rho} \tilde{k} \tilde{u}_j) = \frac{\partial}{\partial x_j} \left[\left(\mu + \frac{\mu_t}{\sigma_k} \right) \frac{\partial \tilde{k}}{\partial x_j} \right] + \bar{G}_k - \bar{\rho} \tilde{\epsilon} \quad (7)$$

$$\begin{aligned} \frac{\partial}{\partial t}(\bar{\rho}\tilde{\epsilon}) + \frac{\partial}{\partial x_j}(\bar{\rho}\tilde{\epsilon}\tilde{u}_j) & \quad (8) \\ & = \frac{\partial}{\partial x_j} \left[\left(\mu + \frac{\mu_t}{\sigma_\epsilon} \right) \frac{\partial \tilde{\epsilon}}{\partial x_j} \right] + \bar{\rho}C_1\tilde{S}\tilde{\epsilon} - \bar{\rho}C_2\frac{\tilde{\epsilon}^2}{\tilde{k} + \sqrt{\nu}\tilde{\epsilon}} + C_{1\epsilon}\frac{\tilde{\epsilon}}{\tilde{k}}C_{3\epsilon}\bar{G}_b \end{aligned}$$

where,

$$C_1 = \max \left[0.43, \frac{\eta}{\eta + 5} \right] \quad (9)$$

$$\eta = \tilde{S} \frac{\tilde{k}}{\tilde{\epsilon}} \quad (10)$$

$$\tilde{S} = \sqrt{2\tilde{S}_{ij}\tilde{S}_{ij}} \quad (11)$$

Finally turbulent viscosity is calculated by Eq. 12.

$$\mu_t = \bar{\rho}C_\mu \frac{\tilde{k}^2}{\tilde{\epsilon}} \quad (12)$$

Ideal gas equation of state (Eq. 13) is used to close the model equations. Note that the flow inside the combustion chamber is assumed to be incompressible since Mach numbers are less than 0.3 within the combustor.

$$\bar{\rho} = \frac{\bar{p}_{op}}{\frac{R}{M_w}\tilde{T}} \quad (13)$$

2.2. Lagrangian Phase Modeling

The atomizer studied is a pressure swirl atomizer which is utilized as a pre-filming air-blast atomizer with the swirler assembly. The thin liquid film formed is neglected and to approximate the film behavior, the droplets normal momentum is reduced accordingly with a coefficient of restitution if it hits the wall.

The primary atomization including film formation and break-up is modeled with the LISA model by Schmidt et al. [4]. For computer memory considerations, secondary breakup is not included in the current study. Parcels represent droplet clusters, and each parcel represents 1000 physical droplets.

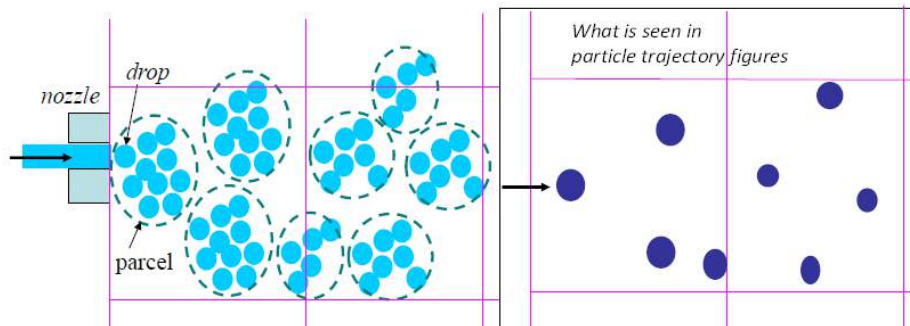


Figure 2: Numerical parcel concept for droplet groups

Forces acting on droplet parcels are considered as per Eq. 15 and Lagrangian parcel trajectories are computed via Eq. 14.

$$\frac{du_{ip}}{dt} = F_D (\tilde{u}_i + u'_i - u_{ip}) \quad (14)$$

$$F_D = \frac{18\mu C_D Re}{\rho_p d_p^2} \frac{1}{24} \quad (15)$$

$$Re = \frac{\rho d_p |\vec{u}_p - \vec{u}|}{\mu} \quad (16)$$

$$C_D = \alpha_1 + \frac{\alpha_2}{Re} + \frac{\alpha_3}{Re} \quad (17)$$

Turbulence droplet interaction needs to be taken into account as well. T_L is a characteristic time scale for this interaction.

$$T_L \approx 0.15 \frac{k}{\epsilon} \quad (18)$$

$$u' = \zeta \sqrt{u'^2}; \quad v' = \zeta \sqrt{v'^2}; \quad w' = \zeta \sqrt{w'^2} \quad (19)$$

ζ appearing in the above equation is a random number with normal distribution. Under the assumption of isotropic turbulence Eq. 19 can be as follows.

$$\sqrt{u'^2} = \sqrt{v'^2} = \sqrt{w'^2} = \sqrt{2k/3} \quad (20)$$

$$\tau_e = -T_L \ln r \quad (21)$$

$$t_{cross} = -\tau \ln \left[1 - \left(\frac{L_e}{\tau |u - u_p|} \right) \right] \quad (22)$$

where,

$$\tau = \frac{\rho_p d_p^2}{18\mu} \quad (23)$$

Due to evaporation of droplets there is mass transfer between two phases. Amount of mass transfer is calculated by Eq. 24.

$$N_i = k_c(C_{i,s} - C_{i,\infty}) \quad (24)$$

$$C_{i,s} = \frac{p_{sat}(T_p)}{RT_p} \quad (25)$$

$$C_{i,\infty} = X_i \frac{P}{RT_\infty} \quad (26)$$

An appropriate Sherwood number correlation is presented in Eq. 27.

$$Sh_{AB} = \frac{k_c d_p}{D_{i,m}} = 2.0 + 0.6 Re_d^{1/2} Sc^{1/3} \quad (27)$$

Parcel mass is updated with Eq. 28.

$$m_p(t + \Delta t) = m_p(t) - N_i A_p M_{w,i} \Delta t \quad (28)$$

Parcel diameter is updated according to Eq. 29.

$$\frac{d(d_p)}{dt} = \frac{4k_\infty}{\rho_p c_p d_p} (1 + 0.23\sqrt{Re_d}) \ln \left[1 + \frac{c_{p,\infty}(\tilde{T}_\infty - T_p)}{h_{fg}} \right] \quad (29)$$

Heat transfer between the droplet phase and gaseous flow is considered as per Eq. 30.

$$m_p c_p \frac{dT_p}{dt} = h A_p (\tilde{T}_\infty - T_p) + \frac{dm_p}{dt} h_{fg} \quad (30)$$

Filming and the break-up of the film surface is represented by the LISA (linearized sheet atomization) model. Mathematical representation of this model for the present simulation is written in Equations 31 through 36.

$$\dot{m}_{eff} = \pi \rho u t (d_{inj} - t) \quad (31)$$

$$\dot{m}_{eff} = \frac{2\pi \dot{m}}{\Delta\phi} \quad (32)$$

$$\Delta\phi = \phi_{stop} - \phi_{start} \quad (33)$$

$$U = k_v \sqrt{\frac{2\Delta p}{\rho_l}} \quad (34)$$

$$k_v = \max \left[0.7, \frac{4\dot{m}_{eff}}{d_0^2 \rho_l \cos \theta} \sqrt{\frac{\rho_l}{2\Delta p}} \right] \quad (35)$$

$$u = U \cos \theta \quad (36)$$

Lastly, there is also momentum exchange between two phases; Eq. 37 describes the amount of force acting on the droplet phase.

$$F = \Sigma \left(\frac{18\mu C_D Re}{\rho_p d_p^2 24} (u_p - \tilde{u}) \right) \dot{m}_p \Delta t \quad (37)$$

2.3 Reaction Mechanism

For the sake of simplicity and computational cost a one-step global mechanism is used to describe chemistry of the reacting flow (Eq. 38). Arrhenius reaction parameters are shown in Table 1.

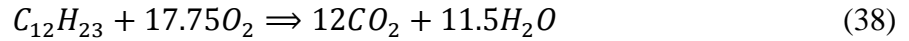


Table 1: Arrhenius parameters.

Parameter	Value	Units
Pre-exponential Constant	2.587e+09	$[m^{1.5}/s kmol^{0.5}]$
Activation Energy	1.256e+08	$[J/kmol]$
Temperature Exponent	0	$[K]$

Parameters related to eddy dissipation concept model are handled in Equations 39 through 41.

$$\zeta^* = C_\zeta \left(\frac{\nu \epsilon}{k^2} \right)^{1/4} \quad (39)$$

$$\tau^* = C_\tau \left(\frac{\nu}{\epsilon} \right)^{1/2} \quad (40)$$

$$R_i = \frac{\rho(\zeta^*)^2}{\tau^*[1 - (\zeta^*)^3]} (Y_i^* - Y_i) \quad (41)$$

2.4 Numerical grid for simulations

The numerical grid consists of $\sim 10^6$ polyhedral elements total for the flame tube and annulus. Figure 3 presents a couple of close up views of the numerical grid.

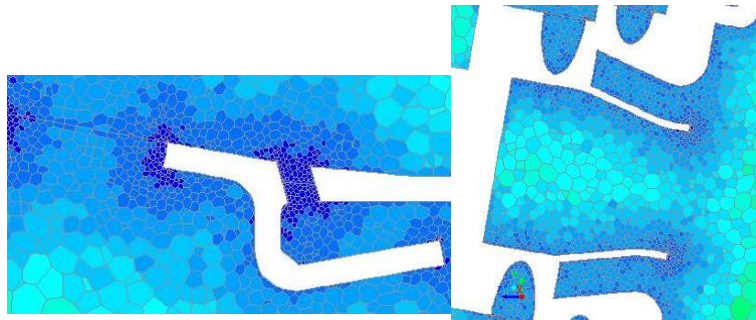


Figure 3: Finite volume grid used in the simulations.

3. Results and Discussion

Boundary conditions for the simulations are presented in Table 2. Note that these figures correspond to on-design-point operating condition of the turboshaft engine.

Table 2 Boundary conditions for numerical simulation.

<i>Inlet</i>	
<i>Mass Flow Rate</i>	<i>0.094 kg/s</i>
<i>Pressure Differential</i>	<i>0 Pa</i>
<i>Turbulence Intensity</i>	<i>10 %</i>
<i>Hydraulic Diameter</i>	<i>18.1 mm</i>
<i>Total Temperature</i>	<i>575 K</i>
<i>N₂ Mass Fraction</i>	<i>0.767</i>
<i>O₂ Mass Fraction</i>	<i>0.233</i>
<i>Outlet</i>	
<i>Pressure Differential</i>	<i>0 Pa</i>
<i>Turbulence Intensity</i>	<i>10 %</i>
<i>Hydraulic Diameter</i>	<i>44 mm</i>
<i>Total Temperature</i>	<i>1370 K</i>
<i>Species Mass Fraction Gradients</i>	<i>0</i>
<i>Injector (for a single injector)</i>	
<i>Mass Flow Rate</i>	<i>0.7 g/s</i>
<i>Temperature</i>	<i>300 K</i>
<i>Internal Pressure</i>	<i>1101325 Pa</i>
<i>Spray Start Angle</i>	<i>0 degree</i>
<i>Spray End Angle</i>	<i>360 degrees</i>
<i>Spray Half Cone Angle</i>	<i>12</i>
<i>Liquid Leaf Constant</i>	<i>0.5</i>
<i>Atomizer Dispersion Angle</i>	<i>12 degrees</i>

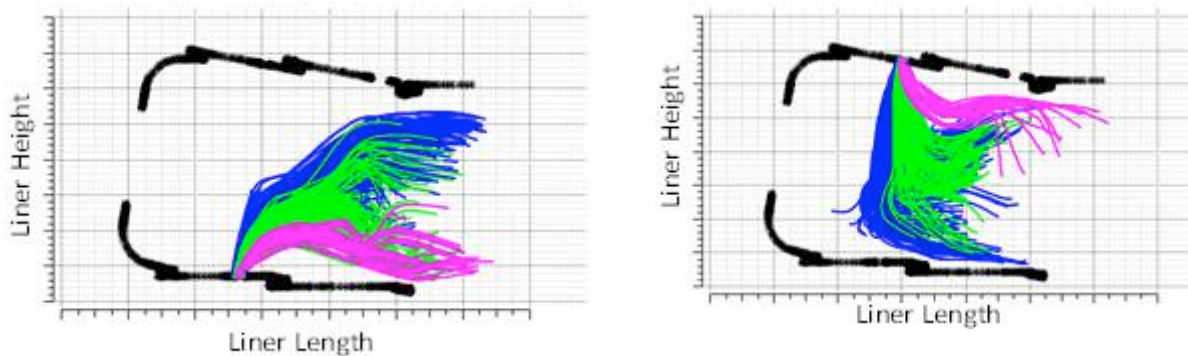


Figure 4: Liner jet trajectories (blue: between the sectors, green: across the injector, purple: beside the injector), inner liner (left) outer liner (right)

Figure 4 presents liner jet trajectories for several cross sections indicated by color-coding. Some of the jets are clearly seen to over penetrate the cross flow reaching up to liner across. Figure 5 demonstrates dynamics of the droplet phase. Figure 6 shows normalized temperature

contours. Normalization is performed with respect to the adiabatic flame temperature. When one considers Figures 5 and 6 simultaneously it is seen that at locations close to the liner walls droplet evaporation and subsequent combustion continues suggesting the possibility over heated liner walls. It might be necessary to resign the combustor features to alter these dynamics.

4. Conclusion

A coupled Euler-Lagrange approach is chosen to simulate the reacting flow field within the reverse flow combustor of a 1000-hp class turboshaft engine. Eddy Dissipation Concept provides meaningful results for the present case. Results indicate that liner walls are subjected to flame (as clearly indicated by Figure 6); therefore a design improvement is necessary should this behavior be consistent with experimental observations. For prospective research experiments are being planned for comparison and validation before changing the geometry of the liner.

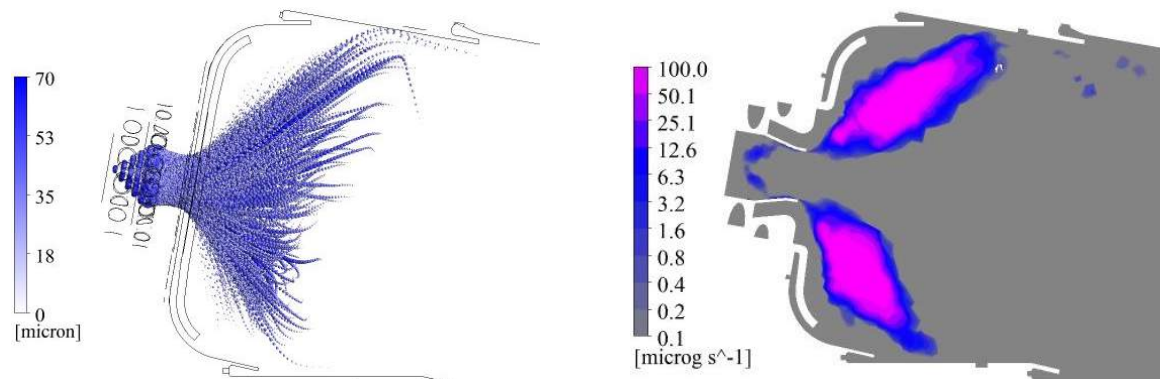


Figure 5: Dynamics of the disperse phase, droplet sizes and trajectories (left) evaporation rate (right)

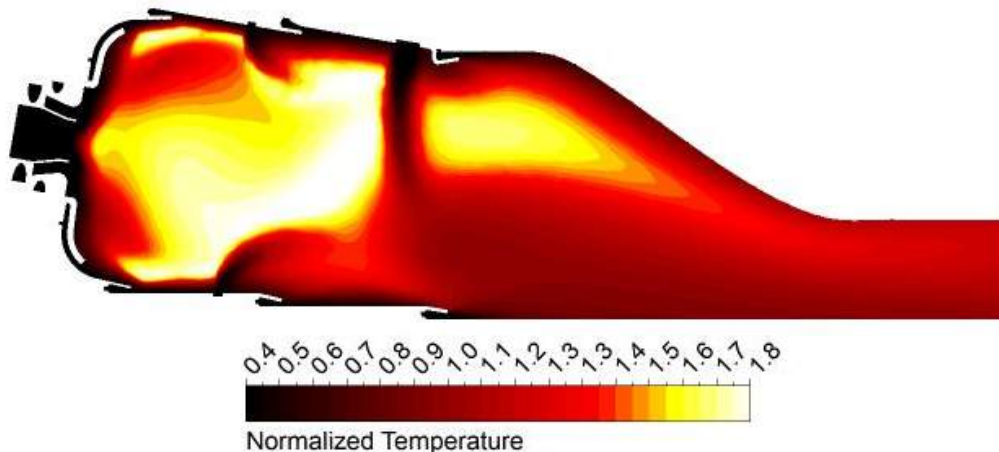


Figure 6: Combustor outlet normalized temperature distribution at the center plane

Acknowledgements

Financial support from the Turkish Ministry of Science, Industry and Technology under contract number 009.STZ.2013-1 is gratefully acknowledged.

References

1. A.H. Lefebvre and D.R. Ballal, Gas Turbine Combustion: Alternative Fuels and Emissions. Taylor and Francis Group, 2010.
2. J.D. Mattingly, Aircraft Engine Design. American Institute of Aeronautics & Astronautics, 2002.
3. I.R. Gran and B.F. Magnussen. A Numerical Study of a Bluff-Body Stabilized Diffusion Flame. Part 2. Influence of Combustion Modeling and Finite-Rate Chemistry. Combust. Sci. Technol., 119: 191–217, 1996.
4. D.P. Schmidt, I. Nouar, P.K. Senecal, C.J. Rutland, J.K. Martin, R.D. Reitz, and J.A. Hoffman. Pressure-Swirl Atomization in the Near Field. SAE Technical Paper No: 1999-01-0496, 1999.